Sanaoi, D. R. (1982) *Biochim. Biophys. Acta 683*, 39–45.
Siegel, J. B., Steinmetz, W. E., & Long, G. L. (1980) *Anal. Biochem. 104*, 160–167.
Stevenson, K. J., Hale, G., & Perham, R. N. (1978) *Biochemistry 17*, 2189–2192.
Stocken, L. A., & Thompson, R. H. S. (1946) *Biochem. J. 40*, 529–535.
Stocken, L. A., & Thompson, R. H. S. (1949) *Physiol. Rev. 29*, 168–194.
Stryer, L., Holmgren, A., & Reichard, P. (1967) *Biochemistry 6*, 1016–1020.
Thelander, L., & Reichard, P. (1979) *Annu. Rev. Biochem. 48*, 133–158.
Voordouw, G., Van der Vies, S. M., Veeger, C., & Stevenson, K. J. (1981) *Eur. J. Biochem. 118*, 541–546.
Whittaker, V. P. (1947) *Biochem. J. 41*, 56–62.
Williams, C. H., Jr., Zanetti, G., Arscott, L. D., & McAllister, J.K. (1967) *J. Biol. Chem. 242*, 5226–5231.

Active-Site Cobalt(II)-Substituted Horse Liver Alcohol Dehydrogenase: Characterization of Intermediates in the Oxidation and Reduction Processes as a Function of pH†

Christian Sartorius,‡ Martin Gerber,‡ Michael Zeppezauer,‡ and Michael F. Dunn*
Department of Biochemistry, University of California, Riverside, California 92521, and Fachbereich Analytische und Biologische Chemie, Universität des Saarlandes, 6600 Saarbrücken, FRG
Received May 12, 1986; Revised Manuscript Received September 18, 1986

ABSTRACT: Substitution of Co(II) for the catalytic site Zn(II) of horse liver alcohol dehydrogenase (LADH) yields an active enzyme derivative, $Co^{II}E$, with characteristic Co(II) charge-transfer and d–d electronic transitions that are sensitive to the events which take place during catalysis [Koerber, S. C., MacGibbon, A. K. H., Dietrich, H., Zeppezauer, M., & Dunn, M. F. (1983) *Biochemistry 22*, 3424–3431]. In this study, UV–visible spectroscopy and rapid-scanning stopped-flow (RSSF) kinetic methods are used to detect and identify intermediates in the LADH catalytic mechanism. In the presence of the inhibitor isobutyramide, the pre-steady-state phase of alcohol (RCH_2OH) oxidation at pH above 7 is characterized by the formation and decay of an intermediate with λ_{max} = 570, 640, and 672 nm for both aromatic and aliphatic alcohols (benzyl alcohol, *p*-nitrobenzyl alcohol, anisyl alcohol, ethanol, and methanol). By comparison with the spectrum of the stable ternary complex formed with oxidized nicotinamide adenine dinucleotide (NAD^+) and 2,2′,2″-trifluoroethoxide ion (TFE^-), $Co^{II}E(NAD^+,TFE^-)$, the intermediate which forms is proposed to be the alkoxide ion (RCH_2O^-) complex, $Co^{II}E(NAD^+,RCH_2O^-)$. The timing of reduced nicotinamide adenine dinucleotide (NADH) formation indicates that intermediate decay is limited by the interconversion of ternary complexes, i.e., $Co^{II}E(NAD^+,RCH_2O^-) \rightleftharpoons Co^{II}E(NADH,RCHO)$. From competition experiments, we infer that, at pH values below 5, NAD^+ and alcohol form a $Co^{II}E(NAD^+,RCH_2OH)$ ternary complex. RSSF studies carried out as a function of pH indicate that the apparent pK_a values for the ionization of alcohol within the ternary complex, i.e., $Co^{II}E(NAD^+,RCH_2OH) \rightleftharpoons Co^{II}E(NAD^+,RCH_2O^-) + H^+$, fall in the range 5–7.5. Using pyrazole as the dead-end inhibitor, we find that the single-turnover time courses for the reduction of benzaldehyde, *p*-nitrobenzaldehyde, anisaldehyde, and acetaldehyde at pH above 7 all show evidence for the formation and decay of an intermediate. Via spectral comparisons with $Co^{II}E(NAD^+,TFE^-)$ and with the intermediate formed during alcohol oxidation, we identify the intermediate as the same $Co^{II}E(NAD^+,RCH_2O^-)$ ternary complex detected during alcohol oxidation.

In recent years, both our understanding of the equine liver alcohol dehydrogenase (LADH,[1] EC 1.1.1.1) catalytic mechanism and our understanding of enzyme catalysis in general have been greatly enriched by the findings of chemists and enzymologists working on LADH [see reviews by Brändén et al. (1975), Dunn (1975, 1984), Klinman (1981), Brändén & Eklund (1980), and Zeppezauer (1983)]. Nevertheless, several aspects of the LADH catalytic mechanism are incompletely resolved: (1) the roles played by protein conformation change are poorly understood; (2) there is no general agreement about the coordination state of the active-site metal during catalysis; (3) there is no agreement about the identities and roles of ionizable groups at the site; and (4) our understanding of elelectrostatic field effects at the site is incomplete.

The most direct evidence indicating that LADH undergoes changes in protein conformation during catalysis is provided

† This work was supported by grants from the Deutsche Forschungsgemeinschaft and the National Science Foundation (DMB-84-08513 and PCM-8108862).
* Address correspondence to this author at the University of California, Riverside.
‡ Universität des Saarlandes.

[1] Abbreviations: E or LADH, horse liver alcohol dehydrogenase; $Co^{II}E$, specifically active-site Co(II)-substituted alcohol dehydrogenase; NAD^+ and NADH, oxidized and reduced nicotinamide adenine dinucleotide, respectively; RCH_2OH and RCH_2O^-, alcohol and alkoxide ion, respectively; RCHO, aldehyde; NBZA and NBZOH, *p*-nitrobenzaldehyde and *p*-nitrobenzyl alcohol, respectively; pyr, pyrazole; IBA, isobutyramide; TFA and TFE^-, 2,2′,2″-trifluoroethanol and 2,2′,2″-trifluoroethoxide ion, respectively; MPD, 2-methyl-2,4-pentanediol; H_2NADH, 1,4,5,6-tetrahydronicotinamide adenine dinucleotide; RSSF, rapid-scanning stopped flow; CME, Cys-46-carboxymethylated LADH; DACA, 4-*trans*-(*N*,*N*-dimethylamino)cinnamaldehyde; LMCT, ligand to metal charge transfer; Bis-Tris, [bis(2-hydroxyethyl)amino]tris(hydroxymethyl)methane; Alc, alcohol; Me_2SO, dimethyl sulfoxide; ADPR, adenine diphosphoribosyl; MES, 2-(*N*-morpholino)ethanesulfonic acid.

0006-2960/87/0426-0871$01.50/0

by the X-ray structures of the native enzyme and of the enzyme–NADH–ligand complexes (Brändén et al., 1975; Samama et al., 1977; Cedergren-Zeppezauer et al., 1982; Eklund et al., 1981; Cedergren-Zeppezauer, 1983). These structures demonstrate that the conformation of LADH depends on interactions with both the coenzyme and the small molecule (substrate or substrate analogue) bound to the substrate site. Two structures appear to be important for catalysis; an "open" conformation characteristic of the orthorhombic form of the crystalline coenzyme-free enzyme (Eklund et al., 1976), and a "closed" conformation characteristic of the triclinic and monoclinic forms of most crystalline ternary complexes (Cedergren-Zeppezauer et al., 1982; Eklund et al., 1982a,b).

There are pronounced differences in conformation between the orthorhombic and triclinic (or monoclinic) forms. Formation of ternary complexes with the closed conformation involves rotation of the catalytic domain relative to the coenzyme binding domain such that water molecules are excluded from the site and the substrate cleft is narrowed to a more closed structure. Within this closed structure, the substrate cleft consists of a polar subsite about the active-site zinc ion that is connected to the surface of the protein by a nonpolar tunnel made up of residues from both subunits. The 1,4-dihydronicotinamide ring of NADH is located in a hydrophobic pocket about 4 Å away from the active-site zinc. There is no obvious counterion contributed by the protein positioned within this subsite to interact with the positively charged nicotinamide ring of NAD^+.

Ternary complex formation is necessary but not always sufficient to trigger the transition from the open to the closed conformation. The X-ray structures of the orthorhombic complexes of E(NADH,imidazole) (Cedergren-Zeppezauer, 1983) and of E(H_2NADH,MPD) (Cedergren-Zeppezauer et al., 1982) both show the open conformation. The orthorhombic complex of MPD, NADH, and Cys-46-carboxymethylated LADH (CME) has a partially closed structure (Cedergren-Zeppezauer et al., 1985). Here, complex formation induces local structural changes in residues 293–297 but does not induce the domain rotation to give the closed conformation.

The structure of the triclinic E(H_2NADH,DACA) complex demonstrates that the water molecule coordinated to zinc ion in the coenzyme-free enzyme is replaced by the carbonyl oxygen of the substrate, whereas in the orthorhombic E-(H_2NADH,MPD) complex, MPD does not coordinate to the metal, but instead seems to be hydrogen bonded to the metal-bound water molecule (Cedergren-Zeppezauer et al., 1982). The DACA complex has the closed conformation while the MPD complex has the open conformation. These observations suggest that inner-sphere coordination of substrate occurs preferentially in the closed conformation. The report that DACA binds exclusively to the triclinic crystals of CME containing NADH and MPD, but not to the orthorhombic species where the conformation is only partially closed, seems to support this suggestion (Cedergren-Zeppezauer, 1985).

The apparent association rate constants for the binding of NAD^+ and NADH to LADH both depend on the protonated form of an enzyme residue with an apparent pK_a of 9.2, whereas the rates of dissociation of NAD^+ and NADH depend respectively on the protonated forms of residues with apparent pK_a's of 7.6 and 11.2 (Kvassman & Pettersson, 1979; Andersson et al., 1981). The binding of DACA to the E(NADH) complex is independent of pH between pH 4 and 10 (Dunn et al., 1975). The binding of ethanol and other alcohols to the E(NAD^+) complex is accompanied by the release of a proton from a group with an apparent pK_a of 6.4. The microscopic origins of these pH dependencies have been the topic of considerable discussion (Shore et al., 1974; Dunn, 1974; Dworschack & Plapp, 1977; Kvassman & Pettersson, 1980b; Klinman, 1981; Makinen et al., 1983; Dietrich et al., 1983). The two most commonly held views are as follows: (a) the pH dependencies which characterize coenzyme binding arise from the ionization of water coordinated to the active-site zinc ion. The pH dependence of alcohol binding arises from the ionization of coordinated alcohol. (b) Alternatively, these pH dependencies involve other residues within the vicinity of the active-site/coenzyme binding site (Bertini et al., 1984; Dietrich et al., 1983; Cook & Cleland, 1981; Cook et al., 1980; Hennecke & Plapp, 1983). The residues which have been suggested include Lys-228 at the anion binding site, the proposed proton relay system involving His-51, or the zinc ligand His-67. The evidence for "cooperative" interactions linking the anion site and ligands coordinated to the active site (Andersson et al., 1980b; Oldén & Pettersson, 1982) implies that the apparent pK_a values associated with ligand and coenzyme binding involve conformational equilibria which are coupled to the ionization of one or more groups.

The chromophoric substrate DACA has been used to probe the microenvironment of the active site (Dunn & Hutchison, 1973; Angelis et al., 1977; Dunn et al., 1982; Dahl & Dunn, 1984a,b). These studies provide strong evidence indicating that within the ternary E–NAD^+–DACA complex the active site of LADH is considerably more polar than water.

The experimental results and conclusions presented in this study are critically dependent on recent developments in three areas which are relevant to the investigation of the LADH catalytic mechanism. They are as follows: (1) the determination of the three-dimensional structures of LADH, LADH complexes, and various LADH derivatives (Brändén et al., 1973, 1975; Samama et al., 1977; Eklund et al., 1981, 1982a,b; Cedergren-Zeppezauer et al., 1982; Cedergren-Zeppezauer, 1983; Schneider et al., 1983); (2) the specific isomorphous substitution of Co^{2+} for Zn^{2+} at the LADH active site (Maret et al., 1979; Dietrich et al., 1979; Schneider et al., 1983); and (3) the detection and investigation of chemical intermediates involved in the LADH catalytic mechanism (Dunn & Hutchison, 1973; Dunn et al., 1982; Koerber et al., 1983).

In the herein presented studies, we make use of the chromophoric properties of active-site-specific Co(II)-substituted LADH to investigate the properties of transient intermediates formed during the interconversion of aliphatic and aromatic aldehydes and alcohols. Via rapid-scanning stopped-flow (RSSF) spectrophotometry in the UV and visible regions (300–700 nm), we have been able to exploit changes in the ligand to metal charge-transfer (LMCT) and d–d electronic transitions of $Co^{II}E$ to directly observe the formation and decay of transient intermediates during a single turnover. The detailed examination of the properties of these intermediates provides new findings which extend our understanding of the roles played by (a) protein conformation, (b) the ionization of coordinated alcohol, and (c) electrostatic force fields in the LADH catalytic mechanism.

Materials and Methods

Buffer solutions were prepared from reagent-grade crystalline salts with deionized, glass-distilled water. All buffers were kept free of chloride ion. Pyrazole and isobutyramide were recrystallized twice in water. The aromatic aldehydes and alcohols were purified by vacuum distillation or sublimation immediately prior to use. NAD^+ (Boehringer, free acid, grade I, 100%) and NADH (Sigma, disodium salt, grade V, 98%) were used without further purification. The exact

concentrations were determined enzymatically prior to use.

LADH was from Boehringer Mannheim, FRG. The active-site Co(II) substitution was carried out by the method of Maret et al. (1979). All preparation, transport, storage, and manipulation of this enzyme derivative took place under nitrogen for protection against oxidative degradation. The crystals of Co(II)-substituted LADH were dissolved in 0.1 M Bis-Tris (pH 6.5). The enzyme active-site concentration, reported as sites occupied by Co(II) ions, was determined spectrophotometrically [see Dunn et al. (1982)]. The occupancy of active sites by Co(II) ions relative to the total protein was found to be between 70% and 85%. Adjustment of all solutions to the desired final pH occurred via pH jump [see Morris et al. (1980)]. The final pH was measured after each experiment.

Routine UV–visible spectral and kinetic data were obtained with a Hewlett-Packard 8450A spectrophotometer. The rapid-scanning stopped-flow (RSSF) spectrophotometry employs a hybrid system consisting of the Durrum D-110 Kel F flow and illumination systems combined with the Princeton Applied Research OMA-2 multichannel analyzer, 1218 controller, and 1412 photodiode array detector together with an external time delay firing circuit to ensure simultaneity of flow stoppage and data acquisition (Koerber et al., 1983). Depending on the region to be studied, the cuvette is illuminated with the full output of either a xenon or a tungsten light source (300–450 or 450–700 nm, respectively). Light exiting from the cuvette is focused on the entrance of a J-Y monochromator modified to function as a polychromator. Pixels are summed and averaged in groups of four to give a wavelength resolution of 2 nm (Koerber et al., 1983). The repetitive scan rate in all experiments was 8.605 ms/scan with time delays introduced between some scans to give the desired scanning sequence. Time-dependent changes of the absorbance at selected single wavelengths were extracted from the complete spectral sets and analyzed via an interactive data reduction program on the Campus VAX 11/750 computer.

RESULTS

Ligand Binding Perturbs the LMCT and d–d Spectral Bands of Co(II)-Substituted LADH. When ligands bind to the coenzyme and to the substrate binding sites, the LMCT and d–d electronic transitions of active-site specifically substituted Co^{II}-LADH undergo characteristic changes in apparent band number, intensity, and position (Maret et al., 1979; Dietrich et al., 1979; Maret, 1980; Andersson et al., 1980a; Dunn et al., 1982; Dietrich & Zeppezauer, 1982; Koerber et al., 1983; Maret & Zeppezauer, 1986). For the studies which follow, the data in Figure 1 serve as a collection of reference spectra which aid in the identification of the intermediates and products formed in the reactions of $Co^{II}E$ with coenzymes, substrates, and inhibitors during a single turnover of enzyme sites.

For aldehyde reduction, limitation of reaction to a single turnover of sites is achieved by including the potent inhibitor pyrazole which reacts rapidly and quasi-irreversibly with enzyme-bound NAD^+ to form a covalent adduct with the nicotinamide ring (McFarland & Bernhard, 1972; Morris et al., 1980; Dunn et al., 1982; Eklund et al., 1982a; Becker & Roberts, 1984). Consequently, during aldehyde reduction, the ternary $Co^{II}E$(NAD–pyr) complex (traces B-1 and C-1, Figure 1) is formed at a rate which is determined by the rate of alcohol desorption from the $Co^{II}E(NAD^+,Alc)$ ternary complex.

For alcohol oxidation, no potent quasi-irreversible inhibitor analogous to pyrazole was available to limit reaction to a single turnover. However, isobutyramide (IBA) binds considerably more tightly in the ternary complex formed with NADH than with NAD^+ and thus makes possible the detection of the pre-steady-state events (Luisi & Bignetti, 1974; Kvassman & Pattersson, 1978). In the presence of IBA, the $Co^{II}E$-(NADH,IBA) ternary complex accumulates (Gerber et al., 1983), and the appearance of the spectrum of this species (traces B-2 and C-2, Figure 1) signals the completion of the pre-steady-state phase of the reaction.

Spectral Changes during Aldehyde Reduction. Figure 2 shows the time-resolved changes in the UV and visible regions (300–700 nm) for the $Co^{II}E$-catalyzed reduction of benzaldehyde at pH 9 (Figure 2A,B) and at pH 5.6 (Figure 2C,D). The insets present "time slices" at selected single wavelengths. These insets also indicate the timing pattern used to collect the scans.

(A) Reaction at High pH. In panels A and B of Figure 2, the entire reaction time course at pH 9.0 is spanned by the set of RSSF spectra numbered 1–18 (Figure 2A-1) and 1–19 (Figure 2B-1). Comparison of spectrum 1 from each data set in Figure 2A,B with the reference spectra in Figure 1 (viz., spectrum C-4) indicates that the initial spectrum of the reacting mixture is dominated by the $Co^{II}E$(NADH,pyr) complex. The absorbance changes for the entire 300–700-nm region occur in two distinct relaxations ($1/\tau_1 > 1/\tau_2$). The spectra collected in these two relaxations are shown respectively as subsets in A-2 and A-3 and B-2 and B-3 of Figure 2A,B. These subsets show that the two relaxations are distinguished from one another by quite different changes. The interconversion of spectral bands in τ_2 generates apparent isoabsorptive points (points of constant absorbance) located at 328 and 374 nm.

During τ_1, an intermediate characterized by a band with λ_{max} = 570 nm appears (viz., subset B-2 of Figure 2B), and there are small intensity changes in the bands located at ~530, ~645, and ~675 nm (decreases). There are apparent isoabsorptive points at ~490, 544, and 615 nm during τ_1. The spectrum of the intermediate (spectrum 7) is nearly identical with the static spectrum of the $Co^{II}E(NAD^+,TFE)$ ternary complex (viz., Figure 6A). During τ_2, the 570-nm band disappears as the spectrum of the $Co^{II}E(NAD^+$–pyr) adduct appears (spectrum 19). The conversion of the 570-nm intermediate to the spectrum of the adduct gives isoabsorptive points at ~465, ~490, ~545, and ~628 nm (subset B-3).

The single-wavelength time courses shown as insets a–d of Figure 2A,B indicate that the rates of the two relaxations associated with intermediate formation and decay are well separated. Time courses measured at 328 and 374 nm (the isoabsorptive points during τ_2) each appear to have the form of a single-exponential decay ($A_t = A_0 \pm A_1[1 - \exp(t/\tau_1)]$) with rate constants ($1/\tau_1$) of approximately 18 ± 2 s^{-1}. At other wavelengths, the time courses are biphasic (viz., the insets at 340, 397, and 670 nm), and depending upon the wavelength selected, these traces appear to consist of the sum of, or difference between, two exponential processes (i.e., compare the time courses at 340, 397, 524, 573, and 670 nm). These time courses were found to be adequately described by the rate law for two, consecutive pseudo-first-order reactions:

$$A_t = A_0 \pm A_1[1 - \exp(t/\tau_1)] \pm A_2[1 - \exp(t/\tau_2)]$$

and analysis of the data gives values of approximately 18 s^{-1} ($1/\tau_1$) and 0.4 s^{-1} ($1/\tau_2$).

The difference spectra shown in Figure 3 illustrate the unique spectral changes which occur in each relaxation by removing background absorbancies contributed by the protein and the unreacted excess of NADH. These difference spectra

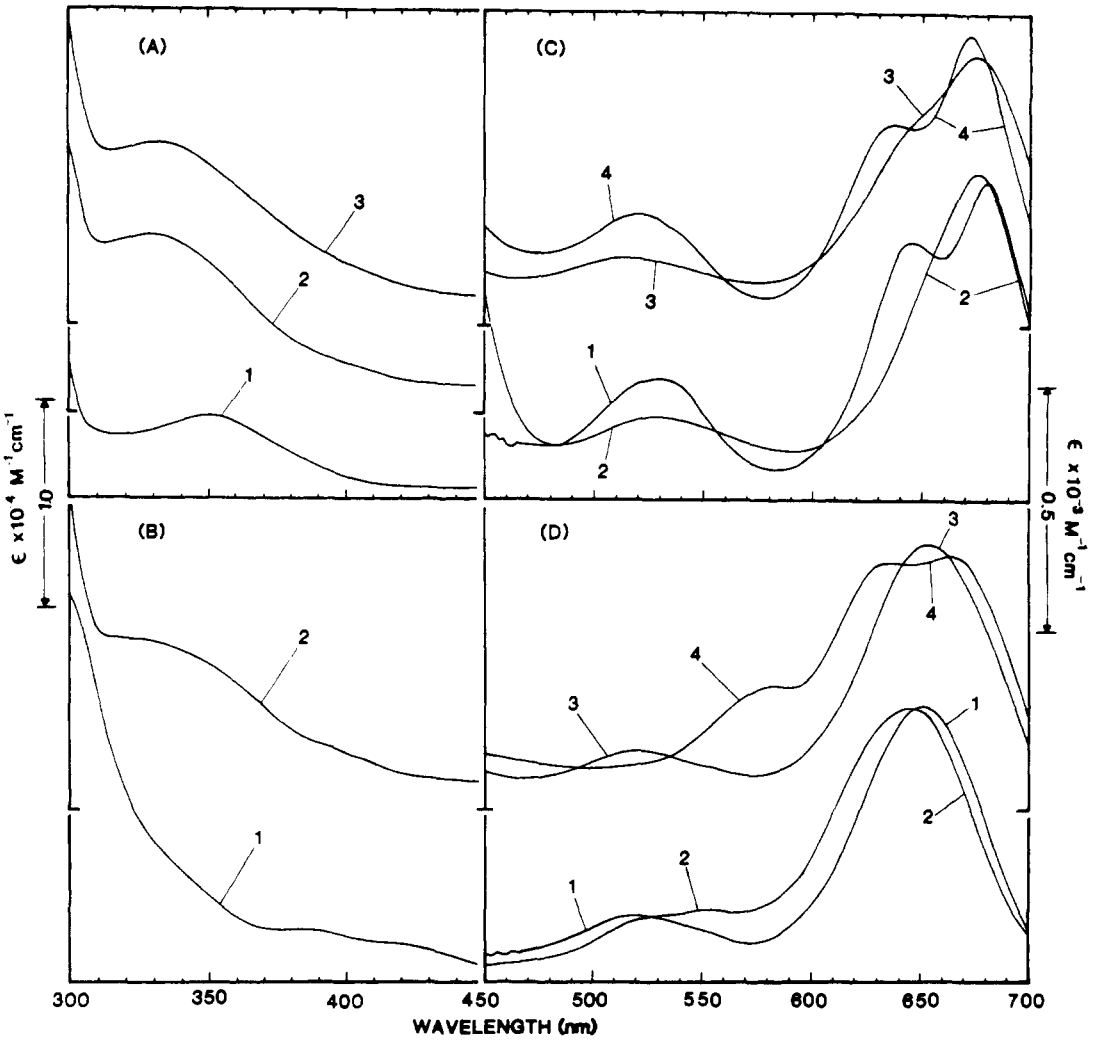

FIGURE 1: Spectra of $Co^{II}E$ complexes at 25 °C. (A and B) 300–450 nm; (C and D) 450–700 nm. A-1, $Co^{II}E$, pH 5.6; A-2, $Co^{II}E$(NADH), pH 9.0; A-3, $Co^{II}E$(NADH,pyr), pH 9. B-1, $Co^{II}E$(NAD–pyr); B-2, $Co^{II}E$(NADH,IBA), pH 9.0. C-1, $Co^{II}E$(NAD–pyr), pH 9; C-2, $Co^{II}E$(NADH,IBA), pH 9.0; C-3, $Co^{II}E$(NADH), pH 9; C-4, $Co^{II}E$(NADH,pyr), pH 9. D-1, $Co^{II}E$, pH 6.3; D-2, $Co^{II}E$, pH 9.0; D-3, $Co^{II}E(NAD^+)$, pH 5.6; D-4, $Co^{II}E(NAD^+)$, pH 9. For clarity in viewing the spectra, each panel is separated by vertical offsets indicated on the ordinates. Spectra were measured with the RSSF spectrophotometer (see Materials and Methods) to take advantage of the time-resolving capabilities of this instrument.

indicate that the spectral changes in τ_1 originate from the disappearance of a species with apparent $\lambda_{max} \simeq 340$ nm. The width of this band and the skewing on the longer wavelength side of the band are indicative that more than one electronic transition is decreasing in this relaxation. Consequently, in agreement with the findings of Koerber et al. (1983), we assign these changes to the oxidation of enzyme-bound NADH (as intermediate is formed) and to changes in at least one cobalt LMCT band located between 330 and 400 nm.

(*B*) *Reaction at Low pH.* In contrast to the behavior at pH 9.0, no intermediates are detected in the reaction of benzaldehyde with the $Co^{II}E$(NADH) complex at pH 5.6 and below. In the wavelength region 300–450 nm (Figure 2C), the spectral changes consist of the concomitant disappearance of bands located between 315 and 395 nm and the appearance of bands below 310 nm and above 400 nm. The crossover points (apparent isosbestic points) located at ~313 and at ~395 nm (see the scale-expanded data set, C-2) are invariant during the entire reaction time course. The changes in the long-wavelength region of the spectrum (450–700 nm, Figure 2D), with apparent isosbestic points at ~638, ~657, and ~680 nm, are relatively small. The band located at 530 nm is essentially unchanged, and the region located between 550 and 700 nm undergoes small changes in intensity and position as the $Co^{II}E$(NADH,pyr) complex (spectrum 1) is converted to the $Co^{II}E$(NAD–pyr) adduct (spectrum 19). When decanoic acid is used in place of pyrazole (Kvassman & Pettersson, 1980a) to inhibit reaction after the first turnover via formation of the $Co^{II}E(NAD^+$,decanoate) complex (data not shown), again no evidence was found for the accumulation of intermediates.

Rapid-scanning studies at pH values intermediate between pH 5.6 and 9.0 (data not shown) establish that the accumulation of intermediate, as measured by the appearance and decay of the 570-, 638-, and 672-nm bands, is pH dependent (viz., Figure 2B); below pH 7.5, the maximum observed amplitude of the 570-nm band decreases with decreasing pH until at pH 5.6 the amount formed is too small to detect (viz., Figure 2D, inset a).

Spectral Changes during Alcohol Oxidation. Sets of time-resolved RSSF spectra and difference spectra at pH values of 9.0, 5.6, and 4.8 for the $Co^{II}E$-catalyzed oxidation of ethanol by NAD^+ in the presence of 50 mM IBA are shown in Figures 4 and 5. Single-wavelength time courses taken from the RSSF data are shown as insets to the figures.

(*A*) *Reaction at High pH.* In the 300–450-nm region (Figure 4A), an envelope of spectral bands dominated by the appearance of bound and free NADH (see below) extending

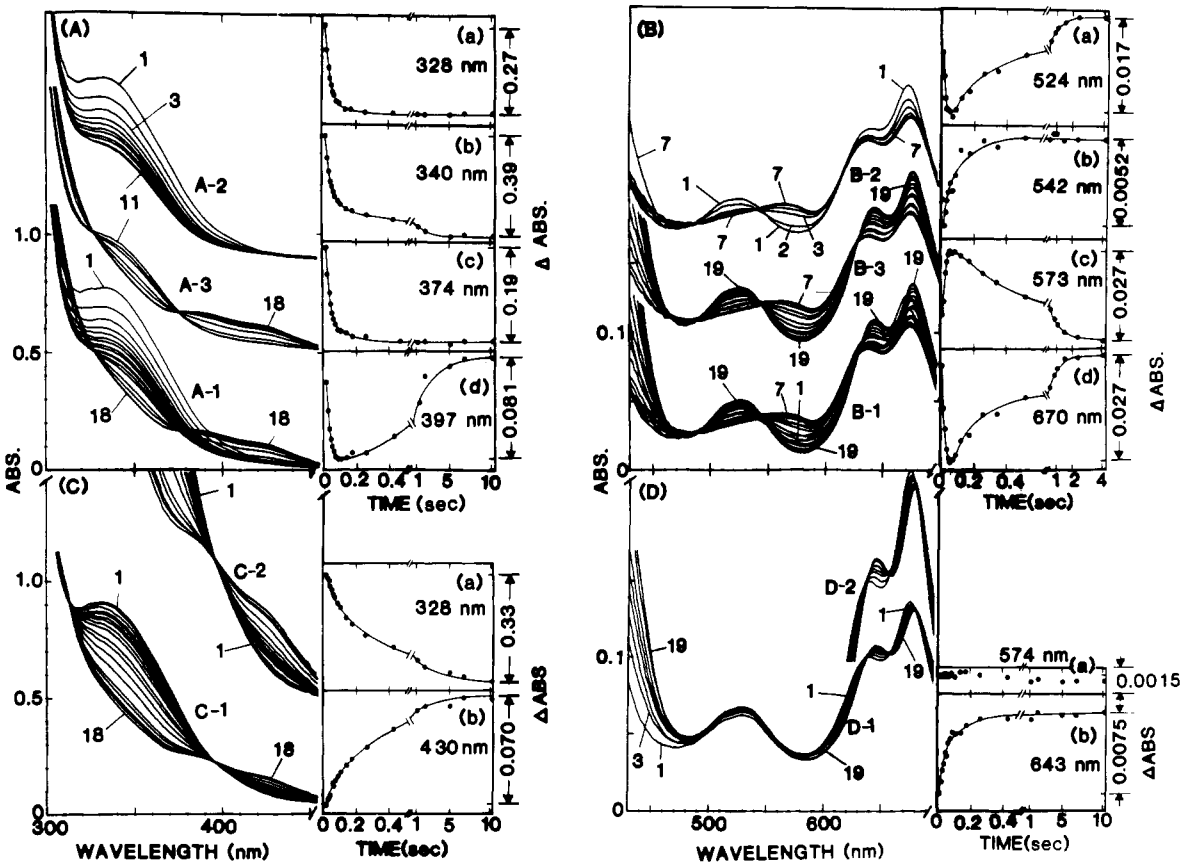

FIGURE 2: Rapid-scanning stopped-flow UV–visible spectra (numbered in chronological order) showing the spectral changes (300–700 nm) that occur during the reduction of benzaldehyde by NADH catalyzed by $Co^{II}E$ at pH 9 (A and B) and pH 5.6 (C and D) and 25 °C. The complete sets of time-resolved spectra for a single turnover are shown respectively in A-1, B-1, C-1, and D-1. To aid in visualizing the spectral changes at pH 9, subsets of spectra for the fast phase (A-2 and B-2) and for the slow phase (A-3 and B-3) are shown offset above the complete sets. In panels C and D, the apparent isosbestic points are shown on expanded scales in C-2 and D-2. Single-wavelength time courses at selected wavelengths are shown at the right side of each panel. Conditions after mixing: (A) $[Co^{II}E]$ = 35 μN; [NADH] = 66.6 μM; [benzaldehyde] = 2 mM; [pyr] = 25 mM; 0.1 M sodium pyrophosphate–50 mM Bis-Tris, final pH 9.0. (B) $[Co^{II}E]$ = 105 μN; [NADH] = 172 μM; [benzaldehyde] = 2 mM; [pyr] = 25 mM; 50 mM glycine hydrochloride–50 mM Bis-Tris, final pH 9.0. (C) $[Co^{II}E]$ = 35 μN; [NADH] = 66.6 μM; [benzaldehyde] = 2 mM; [pyr] = 75 mM; 50 mM sodium citrate–50 mM Bis-Tris, final pH 5.6. (D) $[Co^{II}E]$ = 90 μN; [NADH] = 110 μM; [benzaldehyde] = 2 mM; [pyr] = 75 mM; 0.1 M MES–33 mM Bis-Tris, final pH 5.6. In each experiment, the final pH was achieved by mixing $Co^{II}E$ in pH 6.5 Bis-Tris buffer with NADH, benzaldehyde, and pyr preincubated in a second buffer system (i.e., sodium citrate, MES, glycine, or sodium pyrophosphate as indicated above).

from 300 to 440 nm appears in a burst reaction. The single-wavelength time course at 328 nm shows a fast exponential (pre-steady-state) phase (τ_2*, see below) followed by an approximately zeroth-order (steady-state) phase. The two shoulders present at ~365 and ~400 nm (most easily seen in difference spectra 1–7 of Figure 4C) appear during the burst phase but then undergo very little further change after the steady state is achieved.

The changes in the 450–700-nm region (Figure 5A) consist of (a) a very rapid relaxation (τ_1*) involving the conversion of the $Co^{II}E(NAD^+)$ complex with λ_{max} = 570 and 650 nm to an intermediate with λ_{max} = 570, ~640, and ~672 nm (spectra 1–5) and (b) a slower relaxation (τ_2*, spectra 5–19) involving the replacement of the spectrum of the intermediate by the 525- and 680-nm bands of the $Co^{II}E$(NADH,IBA) ternary complex (viz., Figure 1, spectrum C-2) as the steady state is achieved. The single-wavelength time courses unambiguously establish that the appearance of the 570-nm intermediate (Figure 5A, inset a) occurs more rapidly than does the burst appearance of NADH measured at 328 nm (Figure 4A, inset a). The decay of the 570-nm species (τ_2*) occurs with a rate which is identical (within the limits of experimental error) with the rate of the pre-steady-state burst appearance of NADH in τ_2* measured at 328 nm (compare the insets from Figure 4A with those from Figure 5A). Note that in the 450–700-nm region, the spectrum of the intermediate formed in τ_1* is highly similar to the spectrum of the $Co^{II}E$-(NAD^+,TFE) complex (Figure 6, spectrum A-3).

The difference spectra presented in Figure 4C,D compare the changes which occur in the 300–450-nm region during the pre-steady-state phases of the reaction with the changes which occur in the steady state at both pH 9.0 and pH 4.8. The pre-steady-state changes are evident as negative ΔA (A is absorbance) values while the changes due to formation of free NADH as enzyme turns over in the steady state are evident as positive ΔA values.

(B) pH Dependence of the Benzyl Alcohol Reaction. The pH dependencies of the RSSF time courses were investigated by repeating the RSSF experiments over the pH range 4.8–9.0. As the pH is decreased from 9.0 to 4.8, the rates at which the absorbance changes occur in the 300–450-nm region decrease (compare the RSSF data in panels A and C with those in panels B and D of Figure 4); however, the same envelope of spectral bands extending from 300 to 440 nm appears in the pre-steady-state burst phase, while only the changes due to the production of free NADH are seen in the steady-state phase.

In the 450–700-nm region (Figure 5), the RSSF spectra show there is a pronounced pH dependence of the rates and amplitudes which characterize the reaction. Below pH 7.5,

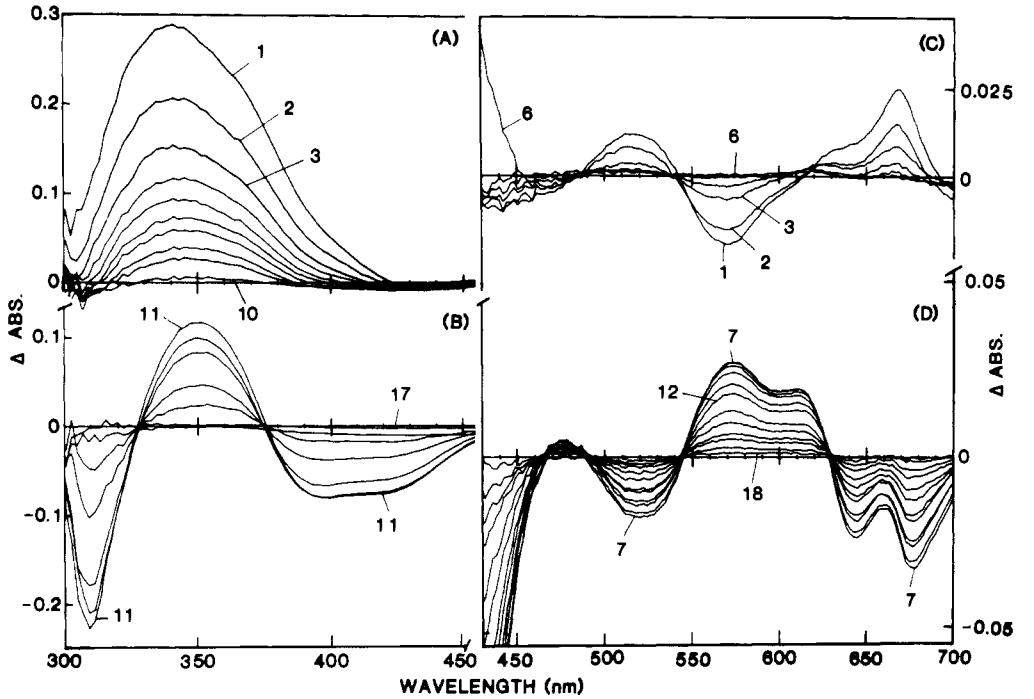

FIGURE 3: Difference spectra (numbered in chronological order) calculated from the data given in Figure 2A,B showing the changes which occur during the fast (A and C) and slow (B and D) relaxations. Difference spectra in (A) were calculated by subtracting spectrum 11 of Figure 2A from spectra 1–10; difference spectra in (C) were calculated by subtracting spectrum 7 of Figure 2B from spectra 1–6. The difference spectra in (B) were calculated by subtracting spectrum 18 of Figure 2A from spectra 11–17; difference spectra in (D) were calculated by subtracting spectrum 18 of Figure 2B from spectra 7–17.

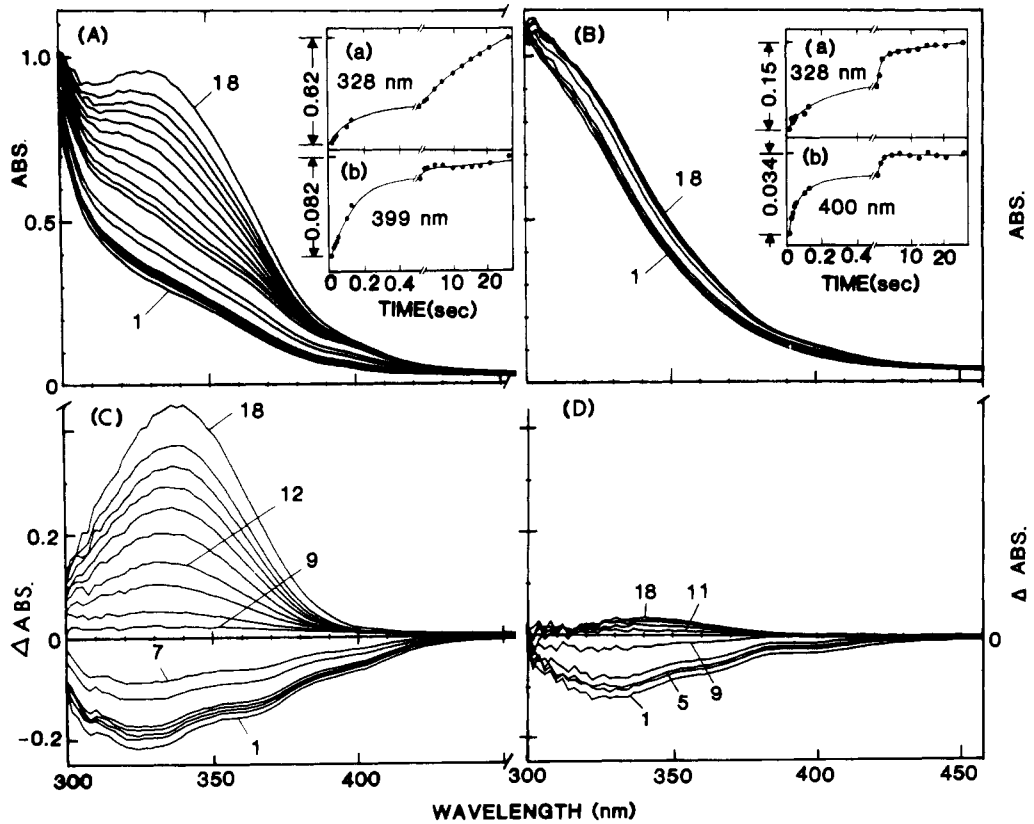

FIGURE 4: Time-resolved spectra and difference spectra for the pre-steady-state and steady-state phases of the $Co^{II}E$-catalyzed oxidation of benzyl alcohol by NAD^+ at pH 9 (A and C) and pH 4.8 (B and D) and 25 °C for the wavelength range 300–450 nm. Difference spectra in (C) and (D) were calculated by subtracting the last spectrum collected in the pre-steady-state phase (respectively spectrum 8 of panel A and spectrum 10 of panel B) from all other spectra in the set. Single-wavelength time courses are shown in insets a and b of panels A and B. Conditions after mixing: (A and C) $[Co^{II}E]$ = 29 μN; $[NAD^+]$ = 1.4 mM; [benzyl alcohol] = 2 mM; [IBA] = 50 mM; 50 mM glycine–50 mM Bis-Tris, final pH 9.0; (B and D) $[Co^{II}E]$ = 29 μN; $[NAD^+]$ = 3.5 mM; [benzyl alcohol] = 4 mM; [IBA] = 50 mM; 10 mM H_2SO_4–50 mM Bis-Tris, final pH 4.8. Reaction was initiated by mixing enzyme in Bis-Tris buffer (pH 6.5) with NAD^+, benzyl alcohol, and IBA preincubated in the above-indicated solutions.

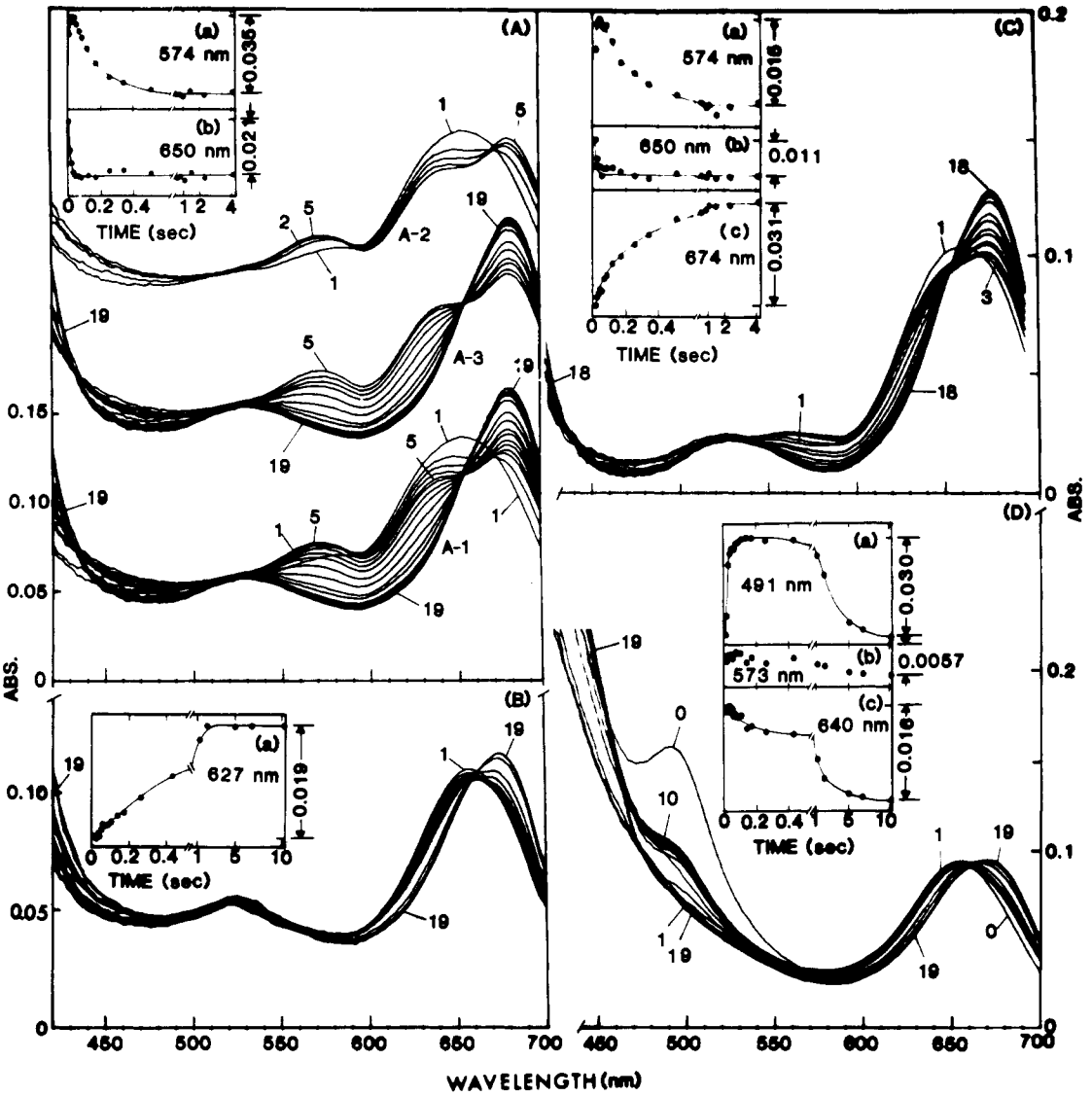

FIGURE 5: Rapid-scanning visible spectra showing the changes in the $Co^{II}E$ spectral bands during the pre-steady-state and steady-state phases of benzyl alcohol oxidation by NAD^+ at pH 9 (A), pH 4.8 (B and D), and pH 5.6 (C) and 25 °C. The pre-steady-state reaction at pH 9 (A) occurs in two kinetic relaxations; the spectra in A-1 show the changes in both relaxations as the steady state is approached; the changes which occur in each relaxation are shown offset in A-2 (the fast relaxation) and A-3 (the slow relaxation), respectively. The time-resolved spectra in (B) and (D) show the changes which occur in the presence (D) and in the absence (B) of a trace of DACA. Spectra 1–19 in (D) are the time-resolved spectra for the reaction of $Co^{II}E$ with NAD^+ and benzyl alcohol in the presence of IBA and DACA. In (D), spectrum 0 is the spectrum of the $Co^{II}E(NAD^+,DACA)$ complex in the absence of benzyl alcohol (but with IBA present) measured in a separate experiment. Conditions after mixing: (A) $[Co^{II}E]$ = 101 μN; $[NAD^+]$ = 1.58 mM; [benzyl alcohol] = 24.1 mM; [IBA] = 45 mM; 50 mM glycine–50 mM Bis-Tris, final pH 9.0. (B) $[Co^{II}E]$ = 89 μN; $[NAD^+]$ = 3.5 mM; [benzyl alcohol] = 4 mM; [IBA] = 50 mM; 10 mM H_2SO_4–50 mM Bis-Tris, final pH 4.8. (C) $[Co^{II}E]$ = 103 μN; $[NAD^+]$ = 3.95 mM; [benzyl alcohol] = 1.8 mM; [IBA] = 45 mM; 7.5 mM H_2SO_4–50 mM Bis-Tris, final pH 5.6. (D) Spectra 1–19: $[Co^{II}E]$ = 108 μN; $[NAD^+]$ = 3.95 mM; [benzyl alcohol] = 4 mM; [DACA] = 4.14 μM; [IBA] = 50 mM; 10 mM H_2SO_4–50 mM Bis-Tris, final pH 4.8. (D) Spectrum 0: conditions are the same as for spectra 1–19 except that no benzyl alcohol is present. Premixing conditions are similar to those described in Figures 2 and 4.

the amount of intermediate with λ_{max} = 570, ~640, and 672 nm formed in τ_1* decreases, and the rate of disappearance of this intermediate decreases (compare panels A, C, and B of Figure 5). At pH 5.6 (Figure 5C), the amount of intermediate formed is small, but still detectable. At pH 4.8 (Figure 5B), the amount of this intermediate is too small to be detected, and the reaction proceeds from an initial spectrum which resembles the $Co^{II}E(NAD^+)$ complex to the spectrum of the $Co^{II}E(NADH,IBA)$ complex without the appearance of the 570-nm band.

The most likely explanations for this pH dependence are as follows: (Case 1) Either the spectrum of the intermediate is pH dependent and/or a different intermediate accumulates. (Case 2) Due to an unfavorable pH dependence for substrate binding, the substrate concentration used is too low to saturate binding and/or reaction. According to case 1, if an intermediate accumulates at pH 4.8 in a process which is faster than the pre-steady-state burst appearance of bound NADH, then the intermediate must have a spectrum in the 450–700-nm region which is nearly the same as that of the $Co^{II}E(NAD^+)$ binary complex.

The predictions for case 1 (above) are borne out by the competition studies presented in Figure 5D. In this experiment, the chromophoric probe DACA is used as an indicator of ligand binding to the active site of $Co^{II}E(NAD^+)$. Dahl and Dunn (1984a) have shown that DACA forms an inner-sphere-coordinated ternary complex, $Zn^{II}E(NAD^+,DACA)$, in which the π,π^* transition of DACA (λ_{max} = 398 nm, ϵ_{max} = 3.15 × 10^4 M^{-1} cm^{-1}) is shifted to 495 nm (ϵ_{max} = 6 × 10^4 M^{-1} cm^{-1}) via coordination of the carbonyl oxygen of DACA to the active-site zinc ion. In the corresponding complex with $Co^{II}E(NAD^+)$, the λ_{max} is shifted to 499 nm (viz., spectrum

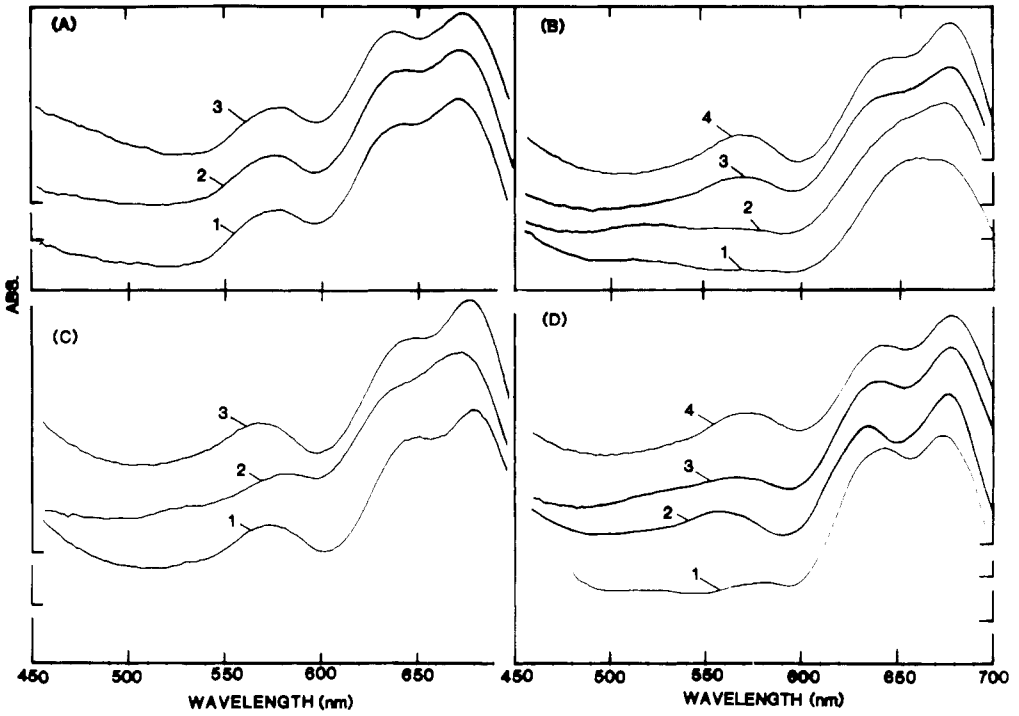

FIGURE 6: Comparison of the spectra of transient intermediates formed during alcohol oxidation (B and C) and aldehyde reduction (D) with the spectrum of the $Co^{II}E(NAD^+,TFE)$ complex (A) in the 450–700-nm region at 25 °C. (A) Spectra of the $Co^{II}E(NAD^+,TFE)$ complex: (1) pH 4.3; (2) pH 6.23; (3) pH 9.0. The spectra shown in (B), (C), and (D) have been selected from RSSF data sets (such as those presented in Figures 2 and 5) to show the maximum amount of 570-nm intermediate. (B) Oxidation of benzyl alcohol: (1) pH 4.8; (2) pH 5.6; (3) pH 6.8; (4) pH 9. (C) Comparison of the transient intermediates formed during the oxidation of (1) *p*-nitrobenzyl alcohol, (2) ethanol, and (3) benzyl alcohol, all at pH 9. (D) Comparison of the transient intermediates formed during the oxidation of (1) acetaldehyde, (2) anisaldehyde, (3) benzaldehyde, and (4) *p*-nitrobenzaldehyde, all at pH 9. The amplitudes of the spectra have been normalized to the same concentration of $Co^{II}E$.

0 of Figure 4D). Since this species is formed rapidly and reversibly but decays to products very slowly, the spectral changes which accompany the competition of DACA with other substrates provide a signal for detecting the binding of other ligands such as benzyl alcohol to the substrate site (as per eq 1–5). If the forward and reverse rate constants for

$$Co^{II}E(NAD^+,DACA)\ (\lambda_{max} = 499\ nm) \underset{k_f}{\overset{k_r}{\rightleftharpoons}} Co^{II}E(NAD^+) + DACA\ (\lambda_{max} = 398\ nm) \quad (1)$$

$$Co^{II}E(NAD^+) + RCH_2OH \rightleftharpoons Co^{II}E(NAD^+,RCH_2OH) \quad (2)$$

$$Co^{II}E(NAD^+,RCH_2OH) \rightleftharpoons Co^{II}E(NAD^+,RCH_2O^-) + H^+ \quad (3)$$

$$Co^{II}E(NAD^+,RCH_2O^-) \rightleftharpoons Co^{II}E(NADH,RCHO) \quad (4)$$

$$Co^{II}E(NADH,RCHO) \rightleftharpoons Co^{II}E(NADH) + RCHO \overset{IBA}{\rightleftharpoons} Co^{II}E(NADH,IBA) \quad (5)$$

DACA binding (k_f and k_r, respectively; eq 1) are rapid relative to the oxidation of benzyl alcohol, and if only a small fraction of the sites are occupied by DACA, then the amplitude of the 499-nm band of the $Co^{II}E(NAD^+,DACA)$ complex will be a simple indicator for benzyl alcohol binding and reaction. The RSSF spectra in Figure 5D compare the spectrum of the $Co^{II}E(NAD^+,DACA)$ complex (spectrum 0) with the set of time-resolved spectra collected under conditions where the same concentrations of $Co^{II}E$, NAD^+, DACA, and IBA are mixed with 4 mM benzyl alcohol, all at a final pH of 4.8. The diminution of the 499-nm spectral band of the DACA complex by approximately two-thirds indicates that 4 mM benzyl alcohol competes with DACA but that this concentration is insufficient to completely saturate the available sites. As oxidation progresses in the first turnover, the residual DACA complex formed in the rapid (preequilibrium) binding step disappears as essentially all pre-steady-state enzyme species are converted to the $Co^{II}E(NADH,IBA)$ complex (spectrum 19 of Figure 5D).

Comparisons with Other Substrates. During the course of these studies, we have also investigated via RSSF UV–visible spectroscopy the reactions of acetaldehyde, anisaldehyde, *p*-nitrobenzaldehyde (NBZA), and cyclohexanone with the $Co^{II}E(NADH)$ complex and the reactions of ethanol, anisyl alcohol, *p*-nitrobenzyl alcohol (NBZOH), and cyclohexanol. The following results (summarized in Figure 6) have been carefully substantiated: (1) The RSSF data for NBZA [see also Koerber et al. (1983)], acetaldehyde, and anisaldehyde (Figure 6D) establish that the spectral changes presented herein for the $Co^{II}E$-catalyzed reaction of NADH with benzaldehyde are characteristic of the behavior of all these substrates. Only the rates of intermediate formation and decay depend upon substrate structure. (2) Although rates depend upon substrate structure, the reactions of ethanol (Figure 6C, spectrum 2), methanol, NBZOH (Figure 6C, spectrum 1), and anisyl alcohol yield intermediates that are very similar to those reported herein for benzyl alcohol (Figure 6B,C, spectrum 3). (3) Due to a highly unfavorable oxido–reduction equilibrium, NBZOH (like TFE) does not proceed appreciably beyond the intermediate formed in τ_1, even in the presence of 50 mM IBA (viz., spectrum 1, Figure 6C). At pH 9, the NBZOH species formed is characterized by λ_{max} located at 570, 645, and 675 nm (essentially the same spectrum given by the TFE ternary complex, compare with the spectra in panel A of Figure 6). At pH 4.8 (data not shown), the NBZOH intermediate, although detectable, appears to be formed in an amount that is less than 10% of the amount which accumulates at pH 9.0. At pH 4.3, this species is no longer detected; however, DACA

displacement studies similar to those reported in Figure 5D indicate a transient $Co^{II}E(NAD^+,NBZOH)$ complex with a spectrum nearly identical with that of $Co^{II}E(NAD^+)$ is formed. (4) The time-resolved spectra which characterize the reactions of cyclohexanone and cyclohexanol (data not shown) are similar to but not identical with the corresponding aldehyde and (primary) alcohol spectra. These spectral charges are sufficiently different to warrant a more detailed treatment and therefore will not be discussed in this report.

Discussion

As will be discussed below, the events which we have thus far detected via changes in the cobalt spectrum of active-site specifically substituted Co^{II}LADH include (a) ligand-induced protein conformation changes, (b) ligand binding, (c) ligand ionization, and (d) hydride transfer. The investigation of these phenomena provides new inferences about the LADH catalytic mechanism pertaining to the roles played by (a) protein conformation change, (b) the active-site microenvironment, and (c) the ionization of inner-sphere-coordinated alcohol.

Interpretation of the Ligand-Induced Perturbations of the d–d Transitions of $Co^{II}E$. The general features of the spectra of $Co^{II}E$ complexes can be summarized as follows: (1) There is a strong correlation between the appearance of bands located between 560 and 580 nm and the inner-sphere coordination of negatively charged ligands (Haas et al., 1986). When bound in ternary complexes with $Co^{II}E$ and NAD^+, decanoate, acetate, azide, cyanide, thiocyanate, and chloride ions all yield bands at ~570 nm which are independent of pH over the range 4–10 (Haas et al., 1986; Maret & Zeppezauer, 1986).

(2) Neutral ligands such as Me_2SO, H_2O, imidazole, pyrazole, isobutyramide, and DACA (Maret et al., 1979; Maret, 1980; Dietrich et al., 1979; Dunn et al., 1982; Haas et al., 1986) yield $Co^{II}E$–ligand binary and/or $Co^{II}E$–coenzyme–ligand ternary complexes which are characterized by a 520–530-nm band (viz., Figure 1).

(3) The 600–700-nm region of the spectrum appears to be sensitive both to changes in protein conformation and to the electronic and/or steric structures of ligands bound to the coenzyme and substrate binding sites. The evidence for a correlation between band position and conformation is as follows: the $Co^{II}E$ (spectra 1 and 2 of Figure 1D) exhibits a broad band with λ_{max} = 645–650 nm; binding of NADH replaces this band, yielding a spectrum with λ_{max} = 675 nm and with a slight shoulder at ~645 nm (spectrum 3 of Figure 1C) (Dietrich et al., 1979; Maret, 1980). High concentrations of ADPR displace NADH with a concomitant shift to a spectrum which is essentially the same as that of $Co^{II}E$ (Maret, 1980; Maret et al., 1984). Single-crystal X-ray diffraction studies show that ADPR binds to the "open" conformation of native enzyme, whereas NADH gives a "closed" conformation (in ternary complexes) (Abdallah et al., 1975). Crystalline native and Co(II)-substituted enzymes have essentially identical structures corresponding to the open conformation (Schneider et al., 1983). The $Zn^{II}E(NADH,MPD)$ and $Co^{II}E(NADH,MPD)$ complexes both have closed structures (E. Cedergren and G. Schneider, personal communication), and $Co^{II}E(NADH,MPD)$ exhibits a 680-nm band with a shoulder at 640 nm. Finally, the $Co^{II}E(NADH,imidazole)$ complex has a 650-nm band (Maret, 1980; Maret et al., 1984). The X-ray structure of the corresponding complex with $Zn^{II}E$ has the open structure (Cedergren-Zeppezauer, 1983).

(4) The similarities in the 600–700-nm region between the spectra of ternary complexes containing both NADH and NAD^+ [compare $Co^{II}E(NADH,pyr)$ with $Co^{II}E(NAD^+,TFE)$ and $Co^{II}E(NAD–pyr)$ (respectively spectra C-4 of Figure 1, A-3 of Figure 6, and C-1 of Figure 1)] indicate this region of the spectrum is insensitive to the charge residing on the nicotinamide ring.

If the above correlations are valid, then the 570-nm bands of the high-pH forms of the $Co^{II}E(NAD^+)$ and $Co^{II}E(NAD^+,TFE)$ complexes are due to the presence of inner-sphere-coordinated anions; therefore, it is difficult to avoid the conclusion that these anions are respectively hydroxide ion and the TFE–alkoxide ion (TFE^-). From their studies of the relationship between alcohol structure and the pH dependence of alcohol binding, Kvassman and Pettersson (1978, 1979, 1980a) and Kvassman et al. (1981) have come to similar conclusions. Since the arguments in support of this intepretation have been cogently presented in their papers, we do not repeat them here.

It is worth considering the possible origins of the spectral change from the acidic to the alkaline form of the binary $Co^{II}E(NAD^+)$ complex. As pointed out by Bertini (Bertini et al., 1982), water and hydroxide are close in the spectrochemical and nephauxelic series, and the ionization of metal-bound water itself is not expected to produce such a significant spectral change at 570 nm. It is therefore more likely that the observed effect of pH, like the introduction of anions in general, reflects a local conformational change in the environment of the catalytic metal ion as a consequence of the charge compensation required by the introduction of a negatively charged species. Thus, there is no direct proof for the existence of a metal-bound hydroxide; the evidence stems solely from the correlation between alcohol structure and the pH dependence of alcohol binding (Kvassman & Pettersson, 1978, 1979, 1980a; Kvassman et al., 1981; these studies) and the similarities in the spectral properties of the $Co^{II}E(NAD^+)$ complex at high pH to the ternary complexes formed between $Co^{II}E,NAD^+$ and anions such as acetate, chloride, and TFE^-.

Finally, because the 650-nm band of $Co^{II}E(NAD^+,H_2O)$ is shifted and split into two bands (with λ_{max} = 645 and 675 nm) when TFE^- displaces H_2O (viz., spectrum D-1 in Figure 1 and spectrum A-2 in Figure 6), we propose that the binding of TFE^- is accompanied by a change in protein conformation which perturbs the geometry of the ligand field and/or the electrostatic environment about the metal ion.

Identification of Intermediates in the $Co^{II}E$-Catalyzed Interconversion of Aldehydes and Alcohols. The RSSF UV–visible absorbance studies presented herein establish that above pH 6 the single-turnover time course for aldehyde reduction involves the formation and decay of a transient intermediate. Due to the large differences in the rates of intermediate formation and decay at pH 9, the RSSF data for benzaldehyde (Figure 2A,B) provide a spectrum for the intermediate which above 400 nm is essentially unperturbed by the presence of other absorbing species. This spectrum is characterized by Co(II) d–d transitions with λ_{max} = 570, 638, and 672 nm and appears nearly identical with the spectrum of $Co^{II}E(NAD^+,TFE^-)$. Due to the presence of excess NADH, we are unable to compare the spectrum of the intermediate to that of $Co^{II}E(NAD^+,TFE^-)$ below 400 nm. Since intermediate formation and NADH oxidation are concomitant processes, we conclude that the intermediate must contain NAD^+ and some form of alcohol bound in a ternary complex. Since the 570-nm band correlates with the inner-shere coordination of an anion, we propose that the intermediate is most likely to be an enzyme–NAD^+–alkoxide ion complex. At pH values below 7, there is a decrease in the amount of intermediate which accumulates; at pH 5.6, we were unable to detect this intermediate with benzaldehyde; however, due to an apparent

difference in pH dependencies, a small amount of this intermediate was detected with *p*-nitrobenzaldehyde below pH 5.6.

At pH values above 5, the pre-steady-state phase of the $Co^{II}E$-catalyzed oxidation of primary alcohols by NAD^+ is also characterized by the formation and decay of a transient intermediate (Figures 4A, 5A, and 6B,C). Under the experimental conditions used, formation of this intermediate is nearly complete within the time required to measure the first spectrum (8–10 ms). Since intermediate decay is a relatively slow process, the nearly unperturbed spectrum of the intermediate is obtained early in the set of time-resolved spectra (e.g., spectrum 3 each of Figures 4A and 5A; see also Figure 6B,C). The spectrum of this intermediate also is characterized by d–d transitions in the long-wavelength region with λ_{max} located at 570, 640, and 672 nm [between 350 and 430 nm, there appear to be changes in a broad envelope of Co(II) LMCT transitions]. Since this species exhibits a 570-nm band and since it forms prior to the appearance of enzyme-bound NADH, again, we conclude that the intermediate must be an enzyme–NAD^+–alkoxide ion complex. Comparison with the spectrum of $Co^{II}E(NAD^+,TFE^-)$ confirms this assignment (Figure 6A).

During the reduction of benzaldehyde, the accumulation of $Co^{II}E(NAD^+,RCH_2O^-)$ is suppressed at pH 5.6, whereas during benzyl alcohol oxidation the pH must be lowered to 4.8 (viz., Figures 5 and 6B) to prohibit the accumulation of this intermediate. We propose that this difference in the amount of $Co^{II}E(NAD^+,RCH_2O^-)$ which accumulates is the consequence of different rates for intermediate formation and decay in the forward and reverse reactions.

At pH values below 5, the DACA displacement studies (viz., Figure 5B,D) strongly indicate that another intermediate exhibiting a spectrum similar to that of the $Co^{II}E(NAD^+)$ complex (with λ_{max} = 525 and 650 nm) accumulates. Since the formation of this intermediate precedes the formation of NADH, we conclude that this intermediate must be an enzyme–NAD^+–alcohol ternary complex. If the 600–700-nm region is a sensitive indicator of protein conformation, as we propose, then the high degree of similarity in the spectra of the low-pH forms of the $Co^{II}E(NAD^+)$ and $Co^{II}E(NAD^+,RCH_2OH)$ complexes is indicative of a high degree of similarity in protein conformation.

From the close similarity of the spectra of intermediates which form during aldehyde reduction to those formed during alcohol oxidation at high pH and to the spectrum of $Co^{II}E(NAD^+,TFE^-)$, we conclude that above pH 6 the same $Co^{II}E(NAD^+,RCH_2O^-)$ complex accumulates irrespective of the direction in which the reaction is run. During alcohol oxidation at low pH, the formation of a second type of $Co^{II}E(NAD^+,RCH_2OH)$ complex with a spectrum highly similar to that of the low-pH form of the $Co^{II}E(NAD^+)$ binary complex strongly implies that the pH dependence of intermediate formation and decay arises from the ionization of the Co(II) inner-sphere-coordinated alcohol and that this ionization triggers a change in conformation of the ternary complex.

Ligand-Induced Protein Conformational Changes in LADH. Ternary complex formation involving enzyme, reduced coenzyme, and substrate (Cedergren-Zeppezauer et al., 1982; Eklund et al., 1982b) or substrate analogues (Eklund et al., 1981, 1982a) causes rotation of the catalytic domain relative to the coenzyme binding domain with a narrowing of the substrate binding cleft and the exclusion of a lattice of solvent water moecules from the vicinity of the active site. So long as the small molecule (substrate or analogue) coordinated to zinc is monodentate, the ligand field retains a distorted tetrahedral geometry (Cedergren-Zeppezauer et al., 1982; Brändén & Eklund, 1980; Zeppezauer, 1983).

Thus far, no unambiguous examples of X-ray structures for binary or ternary complexes with NAD^+ have been published; the E–NAD^+–pyrazole system has been shown to be a convalent adduct wherein N-1 of the pyrazole ring is coordinated to zinc and N-2 is covalently bonded to C-4 of the nicotinamide ring to form a neutral, 1,4-dihydronicotinamide-like structure (Eklund et al., 1982a; Becker & Roberts, 1984). The crystals obtained from solutions of E,NAD^+ and *p*-bromobenzyl alcohol seem to contain a considerable fraction of bound NADH (Eklund et al., 1982b). The same observation was made with the complex crystallized from $Cd^{II}E$, NAD^+, and *p*-bromobenzyl alcohol (Schneider et al., 1985). Nevertheless, single-crystal UV–visible microspectrophotometric studies have shown that the diffusion of aldehydes (e.g., benzaldehyde or acetaldehyde) into monoclinic crystals of the E(NADH,-Me_2SO) complex results in the oxidation of enzyme-bound NADH without disruption of the crystal lattice (Bignetti et al., 1979). This observation suggests that in this crystal there is no pronounced change in protein conformation for the interconversions

$$RCHO + E(NADH,Me_2SO) \rightleftharpoons Me_2SO + E(NADH,RCHO) \rightleftharpoons E(NAD^+,RCH_2O^-) \quad (6)$$

The similarities of the d–d transitions in the 600–700-nm regions of $Co^{II}E$(NADH,pyr), $Co^{II}E$(NAD–pyr), and $Co^{II}E$-(NAD^+,RCH_2O^-) support this suggestion.

The X-ray structural work, the above-mentioned microspectrophotometry, and our RSSF studies all provide evidence which is consistent with the conclusion that the $Co^{II}E$, the $Co^{II}E(NAD^+,H_2O)$, and the $Co^{II}E(NAD^+,RCH_2OH)$ complexes have similar conformations, while the $Co^{II}E(NAD^+,-RCH_2O^-)$ and $Co^{II}E(NAD^+,OH^-)$ complexes have a different conformation. From X-ray diffractions studies (Schneider et al., 1983), it has been established that $Co^{II}E$ crystallizes in the open conformation. The high degree of similarity between the d–d transitions in the 600–700-nm region of $Co^{II}E$, $Co^{II}E(NAD^+,H_2O)$, and $Co^{II}E(NAD^+,RCH_2OH)$ suggests that the open conformation predominates in solution for all three of these structures. If this conclusion is valid, then ionization of inner-sphere-coordinated alcohol or water shifts the conformational equilibria in favor of the closed structure. Therefore, we conclude that a negatively charged metal ligand such as alkoxide ion is necessary for stabilization of the closed conformation in ternary complexes with NAD^+ and enzyme. This is in accordance with conclusions previously drawn from the spectral properties of the $Co^{II}E(NAD^+,Cl^-)$ complex (Maret & Zeppezauer, 1985).

Electrostatic Field Effects at the LADH Active Site. The most reasonable interpretation of the RSSF studies presented in this report is that within the $Co^{II}E(NAD^+,RCH_2OH)$ complex, the pK_a of inner-sphere-coordinated alcohol is strongly perturbed with respect to an aqueous framework of reference. This conclusion is in full accord with both the findings and the conclusions of Kvassman and Pettersson (1978, 1980a) and of Kvassman et al. (1981). From studies of the kinetics and thermodynamics of alcohol binding to the E(NAD^+) complex, they concluded that the pH dependences which characterize alcohol binding arise from the ionizations of inner-sphere-coordinated water and inner-sphere-coordinated alcohol. These two ionizations are sufficient to account for the pH-dependent uptake and release of H^+ during alcohol binding documented by Shore et al. (1974) and by Kvassman et al. (1981). The investigations of Kvassman and Pettersson (1978, 1979, 1980b) and Kvassman et al. (1981) show that

the apparent pK_a values obtained for the ionization of inner-sphere-coordinated alcohols depend on alcohol structure, and a strong correlation between these apparent pK_a values and the pK_a's of these alcohols in aqueous solution was noted. Kvassman et al. (1981) report the following apparent pK_a values for the $E(NAD^+,RCH_2OH)$ ternary complexes: ethanol, 6.4; benzyl alcohol, 6.4; 2-chloroethanol, 5.4; 2,2-dichloroethanol, 4.5; and TFE, 4.3. The apparent pK_a's of inner-sphere-coordinated H_2O in the $Zn^{II}E(NAD^+,H_2O)$, $Zn^{II}E(H_2O)$, and $Zn^{II}E(NADH,H_2O)$ complexes are proposed to be 9.2, 7.6, and 11.2, respectively (Shore et al., 1974; Kvassman & Pettersson, 1979, 1980b; Kvassman et al., 1981). The pK_a values for the $Co^{II}E(H_2O)$ and $Co^{II}E(NAD^+,H_2O)$ complexes are 9.0 and 7, respectively (Sartorius, 1984; Maret & Zeppezauer, 1985). Our RSSF investigations (this work) indicate that for the $Co^{II}E(NAD^+,RCH_2OH)$ systems, the pK_a's of coordinated ethanol, benzyl alcohol, anisyl alcohol, and TFE are similar to the values reported by Kvassman et al. (1981) for the corresponding $Zn^{II}E(NAD^+,RCH_2O^-)$ systems; the pH dependence of the 570-nm band of $Co^{II}E(NAD^+,RCH_2O^-)$ is consistent with pK_a values of about 7 for methanol, 6 for benzyl alcohol, ethanol, and anisyl alcohol, and <4.5 for TFE. All of these pK_a values are lower by several orders of magnitude than the aqueous solution values: H_2O, 15.7; ethanol, 15.9; methanol, 15.5; benzyl alcohol, 15.1; TFE, 12.3 (Ballinger & Long, 1960). Coordination to the active-site zinc ion partially accounts for these perturbed pK_a's; the value of pK_{a_1} for water coordinated to the aquated zinc ion, $Zn^{2+}(H_2O)_6$, is reported as 9.13 (Sillen & Martell, 1964, 1970; Dunn, 1975); pK_a values ranging from 8.7 to 9.3 have been reported for the ionization of H_2O coordinated to small-molecule zinc complexes (Bertini et al., 1980; Billo, 1975; Woolley, 1975). Thus, water coordinated to zinc ion in $Zn^{II}E(H_2O)$, $Zn^{2+}(H_2O)_6$, and in various small-molecule zinc complexes experiences similar pK_a perturbations. The apparent pK_a of coordinated water is raised 2.0 units when NADH binds, a perturbation which is believed to reflect the close proximity and low polarity of the 1,4-dihydronicotinamide ring. Conversely, the apparent pK_a of coordinated water is lowered 1.6 units when NAD^+ binds, and it is probable that this perturbation is largely due to electrostatic effects arising from the close proximity of the positively charged nicotinamide ring.

Although the aqueous solution pK_a values for methanol, ethanol, and benzyl alcohol ($\sim$15–16) are similar to the pK_a of water (15.7), the apparent pK_a values reported for the corresponding $E(NAD^+,RCH_2OH)$ complexes are $\sim$1.5 units lower than the apparent pK_a of $E(NAD^+,H_2O)$. If these apparent values reflect the acidities of the coordinated species, then coordination to the catalytic metal causes larger increases in the acidities of benzyl alcohol and ethanol in comparison to methanol or water. While the origins of this change have not been established, it seems possible that the effect is due to differences in the amount of structured water that remains in the substrate binding cleft. It is likely that in the $Zn^{II}E(NAD^+,H_2O)$ complex, a lattice of hydrogen-bonded water molecules extends from the inner-sphere-coordinated water out through the substrate binding cleft to the bulk solvent. This lattice of water molecules provides a microenvironment which is effective in partially attenuating the electrostatic field generated by Zn(II) and the positively charged nicotinamide ring, and thereby reduces the effect of these charged groups on the pK_a of the coordinated water molecule. If, due to steric constraints, this water lattice is excluded by the hydrocarbon portions of ethanol and benzyl alcohol, then there will be an increase in the net positive electrostatic field experienced by these alcohols. This increased electrostatic field will provide for a greater stabilization of the corresponding alkoxide ions and hence lower pK_a values. The methyl group of methanol may be too small to exclude all of the water from the vicinity of the binding site/catalytic site.

In summary, the UV–visible RSSF experiments presented in this study and the crystallographic work of Brändén et al. (1975), Cedergren-Zeppezauer et al. (1982, 1983), Eklund et al. (1982a,b), and Schneider et al. (1983) indicate that in solution the closed conformations of the $Co^{II}E(NADH,RCHO)$ and $Co^{II}E(NAD^+,RCH_2O^-)$ ternary complexes predominate, whereas the $Co^{II}E(NAD^+,RCH_2OH)$ complex has the open conformation. We postulate two roles in catalysis for the interconversion of the open and closed conformations: (1) ligand binding and dissociation occur via the open conformation, and (2) hydride transfer (eq 7) occurs within the

$$E(NAD^+,RCH_2O^-) \rightleftharpoons E(NADH,RCHO) \qquad (7)$$

closed structure. Due to the exclusion of the lattice of water molecules upon conversion to ternary complexes with the closed conformation, the site microenvironment becomes much more polar. The strong electropositive character of this microenvironment, which derives from the combined electrostatic fields of zinc and NAD^+, stabilizes inner-sphere-coordinated alkoxide ion, the reactive species in alcohol oxidation, while inner-sphere coordination of the aldehyde carbonyl oxygen polarizes the double bond, thus increasing the susceptibility of the carbonyl carbon to hydride attack. Consequently, this highly polar catalytic site solvates the highly polar hydride-transfer transition state, creating an electrostatic strain–distortion effect which results in a low activation energy for hydride transfer.

ACKNOWLEDGMENTS

We thank Drs. Eila Cedergren-Zeppezauer and Gunther Schneider for discussions concerning the relationship between crystal structures and the interconversion of open and closed forms of the various LADH complexes described in the text and for information about some of the complexes prior to publication.

Registry No. NBZOH, 619-73-8; NBZA, 555-16-8; AcH, 75-07-0; $PhCH_2OH$, 100-51-6; EtOH, 64-17-5; MeOH, 67-56-1; PhCHO, 100-52-7; anisyl alcohol, 1331-81-3; anisaldehyde, 50984-52-6.

REFERENCES

Abdallah, M. A., Biellmann, J.-F., Nordström, B., & Brändén, C.-I. (1975) *Eur. J. Biochem. 50*, 475.

Andersson, I., Burton, D. R., Dietrich, H., & Zeppezauer, M. (1980a) in *Metalloproteins* (Weser, U., Ed.) pp 246–253, Thieme-Verlag, Stuttgart, FRG.

Andersson, P., Kvassman, J., Lindström, A., Oldén, B., & Pettersson, G. (1980b) *Eur. J. Biochem. 108*, 303–312.

Andersson, P., Kvassman, J., Lindström, A., Oldén, B., & Pettersson, G. (1981) *Eur. J. Biochem. 113*, 425–433.

Angelis, C. T., Dunn, M. F., Muchmore, D. C., & Wing, R. W. (1977) *Biochemistry 16*, 2922.

Ballinger, P., & Long, F. A. (1960) *J. Am. Chem. Soc. 82*, 785.

Becker, N. H., & Roberts, J. D. (1984) *Biochemistry 23*, 3336–3340.

Bertini, I., Canti, G., Luchinat, C., & Mani, F. (1980) *Inorg. Chim. Act 46*, 291.

Bertini, I., Luchinat, C., & Scozzafava, A. (1982) *Struct. Bonding (Berlin) 48*, 46–91.

Bertini, I., Gerber, M., Lanini, G., Luchinat, C., Maret, W., Rawer, S., & Zeppezauer, M. (1984) *J. Am. Chem. Soc. 106*, 1826.

Bignetti, E., Rossi, G. L., & Zeppezauer, E. (1979) *FEBS Lett. 100*, 17–22.
Billo, E. J. (1975) *Inorg. Nucl. Chem. Lett. 11*, 491.
Brañdén, C.-I., & Eklund, H. (1980) in *Dehydrogenases Requiring Nicotinamide Coenzyme* (Jeffrey, J., Ed.) Birkhauser Verlag, Basel, Switzerland.
Brändén, C.-I., Eklund, H., Nordström, B., Boiwe, T., Söderlund, G., Zeppezauer, E., Ohlsson, I., & Åkeson, Å. (1973) *Proc. Natl. Acad. Sci. U.S.A. 70*, 2439.
Brändén, C.-I., Jörnvall, H., Eklund, H., & Furugren, B. (1975) *Enzymes (3rd Ed.) 11*, 103–190.
Cedergren-Zeppezauer, E. (1983) *Biochemistry 22*, 5761.
Cedergren-Zeppezauer, E., Samama, J.-P., & Eklund, H. (1982) *Biochemistry 21*, 4895–4908.
Cook, P. F., & Cleland, W. W. (1981) *Biochemistry 20*, 1805.
Cook, P. F., Blanchard, J. S., & Cleland, W. W. (1980) *Biochemistry 19*, 4853–4858.
Dahl, K. H., & Dunn, M. F. (1984a) *Biochemistry 23*, 4094–4100.
Dahl, K. H., & Dunn, M. F. (1984b) *Biochemistry 23*, 6829–6839.
Dietrich, H., & Zeppezauer, M. (1982) *J. Inorg. Biochem. 17*, 227–235.
Dietrich, H., Maret, W., Wallén, L., & Zeppezauer, M. (1979) *Eur. J. Biochem. 100*, 267–270.
Dietrich, H. MacGibbon, A. K. H., Dunn, M. F., & Zeppezauer, M. (1983) *Biochemistry 22*, 3432–3438.
Dunn, M. F. (1974) *Biochemistry 13*, 1146–1151.
Dunn, M. F. (1975) *Struct. Bonding (Berlin) 23*, 61–122.
Dunn, M. F. (1984) in *Enzymology of Carbonyl Metabolism: Aldehyde Dehydrogenase and Aldo/Keto Reductase*, Vol. II, pp 151–168, Alan R. Liss, New York.
Dunn, M. F., & Hutchison, J. S. (1973) *Biochemistry 12*, 4882–4892.
Dunn, M. F., Biellmann, J.-F., & Branlant, G. (1975) *Biochemistry 14*, 3176.
Dunn, M. F., Dietrich, H., MacGibbon, A. K. H., Koerber, S. C., & Zeppezauer, M. (1982) *Biochemistry 21*, 354–363.
Dworschack, R. T., & Plapp, B. M. (1977) *Biochemistry 16*, 111.
Eklund, H., Nordström, B., Zeppezauer, E., Söderlund, G., Ohlsson, I., Bowie, T., Söderburg, B.-O., Tapia, O., Brändén, C.-I., & Åkeson, Å. (1976) *J. Biol. Chem. 102*, 27–59.
Eklund, H., Samama, J.-P., Wallén, L., Brändén, C.-I., Åkesson, Å., & Jones, T. A. (1981) *J. Mol. Biol. 146*, 561–587.
Eklund, H., Samama, J.-P., & Wallén, L. (1982a) *Biochemistry 21*, 4858.
Eklund, H., Plapp, B. V., Samama, J.-P., & Brändén, C.-I. (1982b) *J. Biol. Chem. 257*, 14349.
Gerber, M., Zeppezauer, M., & Dunn, M. F. (1983) *Inorg. Chim. Acta 79*, 161–164.
Haas, C., Maret, W., Zeppezauer, M., Lanini, G., Luchinat, C., & Bertini, I. (1987) *Eur. J. Biophys.* (in press).
Hennecke, M., & Plapp, B. V. (1983) *Biochemistry 22*, 3721–3728.
Klinman, J. P. (1981) *CRC Crit. Rev. Biochem. 10*, 39.
Koerber, S. C., MacGibbon, A. K. H., Dietrich, H., Zeppezauer, M., & Dunn, M. F. (1983) *Biochemistry 22*, 3424.
Kvassman, J., & Pettersson, G. (1978) *Eur. J. Biochem. 87*, 417.
Kvassman, J., & Pettersson, G. (1979) *Eur. J. Biochem. 100*, 115–123.
Kvassman, J., & Pettersson, G. (1980a) *Eur. J. Biochem. 103*, 557–564.
Kvassman, J., & Pettersson, G. (1980b) *Eur. J. Biochem. 103*, 565–575.
Kvassman, J., Larsson, A., & Pettersson, G. (1981) *Eur. J. Biochem. 114*, 555.
Luisi, P. L., & Bignetti, E. (1974) *J. Mol. Biol. 88*, 653–670.
Makinen, M. W., Maret, W., & Yim, M. B. (1983) *Proc. Natl. Acad. Sci. U.S.A. 80*, 2584–2588.
Maret, W. (1980) Doctoral Dissertation, Universität des Saarlandes, Saarbrucken, FRG.
Maret, W., & Zeppezauer, M. (1986) *Biochemistry 25*, 1584–1588.
Maret, W., Anderson, I., Dietrich, H., Schneider-Berhlöur, H., Einarsson, R., & Zeppezauer, M. (1979) *Eur. J. Biochem. 98*, 501–512.
Maret, W., Gerber, M., Zeepezauer, M., & Dunn, M. F. (1984) in *Enzymology of Carbonyl Metabolism: Aldehyde Dehydrogenase and Aldo/Keto Reductase*, Vol. II, pp 181–191, Alan R. Liss, New York.
McFarland, J. T., & Bernhard, S. A. (1972) *Biochemistry 11*, 1486–1493.
Morris, R. G., Saliman, G., & Dunn, M. F. (1980) *Biochemistry 19*, 725–731.
Oldén, B., & Pettersson, G. (1982) *Eur. J. Biochem. 125*, 311–315.
Samama, J.-P., Zeppezauer, E., Biellmann, J.-F., & Brändén, C.-I. (1977) *Eur. J. Biochem. 81*, 403–409.
Sartorius, C. (1984) Diploma Thesis, Universität des Saarlandes, Saarbrücken, FRG.
Schneider, G., Eklund, H., Cedergren-Zeppezauer, E., & Zeppezauer, M. (1983) *Proc. Natl. Acad. Sci. U.S.A. 80*, 5289.
Schneider, G., Cedergren-Zeppezauer, E., Knight, S., Eklund, H., & Zeppezauer, M. (1985) *Biochemistry 24*, 7503–7510.
Shore, J. D., Gutfreund, H., Brooks, R. L., Santiago, D., & Santiago, P. (1974) *Biochemistry 13*, 4185.
Sillen, L. G., & Martell, A. E. (1964) in *Stability Constants of Metal-Ion Complexes*, Part II, The Chemical Society, Burlington House, London.
Sillen, L. G., & Martell, A. E. (1970) in *Stability Constants of Metal-Ion Complexes*, Part III, The Chemical Society, Burlington House, London.
Woolley, P. (1975) *Nature (London) 258*, 675.
Zeppezauer, M. (1983) *NATO ASI Ser., Ser. B 100*, 99.